THE ATMOSPHERES OF A-TYPE SUBDWARFS AND 95 LEONIS*

JOSEPH W. CHAMBERLAIN AND LAWRENCE H. ALLER
Observatory, University of Michigan
Received February 14, 1951

ABSTRACT

Line profiles and equivalent widths have been measured in the spectra of two subdwarfs, HD 19445 and HD 140283, classified as A4sp and A5sp, and a main-sequence A4 star, 95 Leonis. The data are analyzed by conventional curve-of-growth procedures and by the method of model atmospheres and line profiles. The point of view adopted is that the structure of the atmosphere must correctly reproduce the profiles of the hydrogen lines. It is found that for 95 Leonis $T_{\text{eff}}=8900^\circ$ K and $\log g \simeq 3.90$ (which are normal for an A4 star), whereas for the subdwarfs $T_{\text{eff}} = 6300^\circ$ K and $\log g \simeq 4.80$.

The assumption that the amount of hydrogen per gram of stellar material is the same as that in the sun is in harmony with the data; i.e., there is no evidence that the subdwarfs are deficient in hydrogen. The excitation temperatures are derived from curves of growth for *Fe* I, using King's laboratory *f*-values. A comparison of theoretical and observed line profiles and equivalent widths suggests that *Ca* is deficient in the subdwarf atmospheres. Low *Fe* abundances in these stars are indicated by curves of growth constructed with Greenstein's empirical line strengths for τ UMa and υ Sgr. The color temperatures and the Balmer discontinuities are predicted.

I. INTRODUCTION

The stars HD 19445 and HD 140283 are listed in the Mount Wilson Spectroscopic Parallax Catalogue[1] with absolute magnitudes intermediate between the main-sequence A stars and the conventional white dwarfs. These "intermediate white dwarfs" or "subdwarfs" possess a number of interesting spectral peculiarities. The spectral classification given in the *Henry Draper Catalogue*, which is based essentially on the Balmer lines, differs considerably from that listed by the Mount Wilson observers, who classified the spectra without regard to the appearance of the hydrogen lines. The presence of relatively sharp and weak hydrogen lines, in what otherwise might be classed as A-type spectra, is perhaps the most interesting observed feature of the subdwarfs.

95 Leonis (HD 103578) is apparently a normal A star lying slightly above the main sequence of the Hertzsprung-Russell diagram. Table 1 summarizes the available information on these stars.

An interpretation of the subdwarf spectra must necessarily predict either (1) a chemical composition similar to that of the sun, with the peculiarities explained in terms of the physical parameters of the star's atmosphere; (2) an actual surplus or deficiency of one or more elements; or (3) a combination of anomalous abundances *and* physical conditions. In turn, the hydrogen/metal ratio may be abnormal, or the metals may show relative abundances different from those of the solar atmosphere. Kuiper[2] has suggested that the subdwarfs and the high-velocity stars in general might have low hydrogen contents.

No quantitative analysis of the spectra of A-type subdwarfs has heretofore been attempted. The object of this paper is to show that these spectra may be explained in terms of atmospheres that have temperatures appropriate to F-type stars and that are not deficient in hydrogen. Certain metals do appear to have abnormally low abundances, however. We will also attempt to show that several features of the spectrum of 95 Leonis can be reproduced theoretically on the assumption of normal solar abundances and a model atmosphere representing a star that is slightly above the main sequence.

* This investigation was made possible by a co-operative arrangement between the University of Michigan and the Mount Wilson and Palomar Observatories.

[1] *Ap. J.*, **81**, 187, 1935. [2] *A.J.*, **53**, 194, 1948.

In Section III we discuss the determination of the excitation temperature with the aid of King's laboratory *f*-values and conclude that the temperatures for the subdwarfs are much lower than for ordinary A stars. Similarly, Verweij's theoretical hydrogen profiles, when compared with the observed profiles, indicate either extremely low surface gravities (which seems doubtful) or low temperatures. Preliminary values for the surface gravities and effective temperatures of these stars are derived in Section IV from curve-of-growth considerations. T_{eff} and g are then used to construct provisional model atmospheres, which, in turn, serve as the starting point for the calculation of theoretical line profiles for hydrogen (Sec. V) and for λ 3933 and λ 4227 of *Ca* (Sec. VI). The correct prediction of line profiles and equivalent widths is a necessary condition for acceptable model atmospheres. Thus, to obtain the final model atmospheres, we use the trial-and-error method of assuming T_{eff} and g, calculating a model atmosphere, and then predicting line profiles, which are compared with the observations. The adopted atmospheric structure not only should yield the correct profiles but also should predict the

TABLE 1

DATA FOR 95 LEONIS AND SUBDWARFS

Star	α (1900)	δ (1900)	Spectral Type		M_{vis} Mt. W.
			HD	Mt. W.	
95 Leonis (HD 103578)....	$11^{h}50^{m}.5$	+16°12′	A2	A4s	+1.2
HD 19445.....	3 2.5	+25 59	F2	A4sp	+5.0
HD 140283.....	15 37.7	−10 36	F5	A5sp	+4.9

Star	m_{vis}	Rad. Vel.	μ_α	μ_δ
95 Leonis (HD 103578)....	5.49	(Var.) $v_0 = -21.$km	+0″010	−0″007
HD 19445.....	8.0	−143.	−0.222	− .796
HD 140283.....	7.26	−171.0	−1.666	−0.320

observed color temperature and Balmer discontinuity (Sec. VIII). In a word, it must explain all the observed data. Curves of growth for *Fe*, based on Wrubel's theoretical curve, are given in Section VII. Empirical line strengths obtained from stars other than the sun seem to be most satisfactory for our purposes. The curve-of-growth results, however, definitely seem to be less reliable than those obtained from line profiles.

II. OBSERVATIONAL DATA

One plate of each of the subdwarfs and two of 95 Leonis were made with the coudé grating spectrograph and 32-inch camera at the 100-inch telescope of the Mount Wilson Observatory. This combination gives a normal dispersion of about 10 A/mm. Tracings of the plates were made with the conventional transmission-type microphotometer in Pasadena, with a magnification of 60 × plate. Photometric calibration was supplied by a step-slit.

The coudé plates were supplemented with two exposures of 95 Leonis made with the 24-inch camera attached to the two-prism spectrograph of the 37½-inch reflector in Ann Arbor. The dispersion is 20 A/mm at $H\gamma$. The emulsion employed was Eastman II*a*-O, and the plates were calibrated with a wedge-slit calibration spectrograph, which is de-

scribed elsewhere.[3] Tracings with a magnification of 49× were made of the hydrogen and H and K lines with the Moll microphotometer at Ann Arbor.

Figure 1 illustrates the discrepancy in the observed profiles as obtained from the grating and prism spectrographs. It seems reasonable to suppose that the difference is due primarily to scattering of light in the grating spectrograph. Assuming that the amount of light scattered by the prism instrument in the direction of the plate is negligible, we have compared the observed equivalent widths of $H\beta$, $H\gamma$, and $H\delta$ to obtain an estimate of the amount of grating scattering. A mean value of about 25 per cent was obtained, with good agreement among the separate determinations. Applying this correction to the hydrogen and K-line profiles obtained from the grating spectra, we obtained good fits with the prism profiles. This estimate of the scattering is in accordance with some previous determinations for this Mount Wilson grating.[4]

On the assumption that the amount of scattering is the same in all regions of the spectrum and in all the grating plates used, we have applied the above correction to all grating equivalent widths and profiles. A systematic error of a few per cent in this correction should make very little difference in the final results.

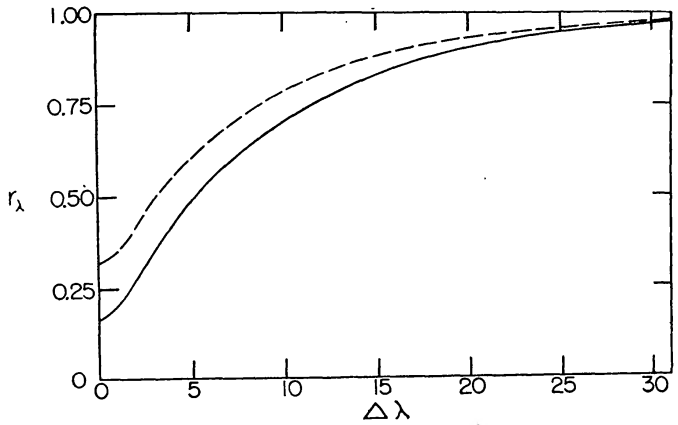

FIG. 1.—Effect of scattering produced by grating spectrograph. *Solid curve*, prism profile; *dashed curve*, uncorrected grating profile. Curves are for $H\gamma$ in 95 Leonis.

In general, there is good agreement between the equivalent widths obtained from the two grating plates of 95 Leonis. However, the central portions of the very strongest lines differ somewhat in the two cases. This is probably due to small errors in the toe of the characteristic curve, where a small change in plate density corresponds to a rather large factor on the intensity scale.

The measured grating intensities for the *Fe* I and *Fe* II lines are listed in Table 2, together with the wave length and excitation potential of the lower level for each line. As we will explain in Section VII, only lines in the λλ 4000–4800 region could be used in the final curve of growth. Lines falling in the wing of a hydrogen line were also omitted.

III. THE EXCITATION TEMPERATURE

For the determination of the excitation temperature of a star from equivalent widths, approximate values of the stellar temperature and of the damping constant for the lines utilized are necessary. Rough values of the damping constant can be determined if preliminary estimates of the effective temperature and surface gravity are available. From the spectral type of 95 Leonis we took $T_{\rm eff} = 8900°$ K and $\log g = 4.30$, whereas the peculiarities of the subdwarf spectra make such estimates impracticable.

[3] R. C. Williams, *Pub. Obs. U. Michigan*, **7**, 93, 1938. [4] L. H. Aller, *Ap. J.*, **96**, 321, 1942.

TABLE 2

EQUIVALENT WIDTHS OF IRON ABSORPTION LINES
(Uncorrected Grating Intensities)

λ	IDENTIFICATION	W(mA)			E.P. (VOLTS)
		95 Leonis	HD 19445	HD 140283	
4063.61	*Fe* I	80	106	96	2.95
4067.99	I	22	23	8	1.80
4071.76	I	78	115	107	3.28
4122.64	II	42	.....	.....	2.57
4128.75	II	19	.....	.....	2.57
4132.04	I	52	68	68	1.60
4132.97	I	.....	15	23	2.82
4143.37	I	46	51	39	2.20
4143.87	I	68	78	68	2.67
4157.80	I	53	.....	37	1.90
4173.47	II	87	37	33	2.57
4175.60	I	36	39	71	1.85
4178.85	II	73	34	.....	2.57
4184.93	I	9	.....	.....	1.70
4187.02	I	52	56	35	2.40
4187.81	I	44	58	52	3.05
4210.31	I	35	.....	.....	2.07
4216.19	I	50	.....	.....	0.00
4219.41	I	33	.....	.....	3.56
4222.23	I	42	.....	.....	2.44
4227.41	I	58	58	35	3.32
4233.18	II	89	49	32	2.57
4233.61	I	42	33	38	2.47
4235.92	I	51	83	76	2.42
4247.41	I	25	.....	.....	3.35
4248.16	I	14	.....	.....	3.06
4250.10	I	45	43	.....	2.46
4250.78	I	50	89	.....	1.55
4260.46	I	60	72	72	2.39
4271.16	I	48	72	30	2.44
4271.76	I	60	110	50	1.48
4273.32	II	56	.....	19	2.69
4282.41	I	27	39	34	2.17
4296.56	II	44	.....	26	2.69
4303.16	II	62	.....	.....	2.69
4351.71	II	.....	104	.....	2.69
4369.41	II	39	.....	.....	2.77
4383.53	I	70	123	83	1.48
4385.38	II	77	.....	.....	2.77
4388.41	I	20	.....	.....	3.59
4404.74	I	68	98	63	1.55
4415.08	I	61	72	51	1.60
4416.80	II	64	.....	.....	2.77
4427.32	I	22	54	59	0.05
4430.62	I	19	.....	26	2.21
4442.35	I	26	41	.....	2.19
4447.71	I	49	.....	23	2.21
4466.55	I	42	51	17	2.82
4472.90	II	45	.....	.....	2.83
4476.09	I	41	33	24	2.83
4489.15	II	62	.....	.....	2.82
4491.36	II	62	.....	.....	2.84
4494.51	I	50	.....	.....	2.19
4508.26	II	68	50	.....	2.84
4515.31	II	70	.....	.....	2.83
4520.21	II	100	.....	.....	2.80
4522.59	II	88	47	.....	2.83
4541.50	II	42	.....	.....	2.84
4555.84	II	77	15	18	2.82
4576.25	II	35	.....	.....	2.83
4582.75	II	30	.....	.....	2.83
4583.79	II	59	28	.....	2.80
4620.48	II	60	.....	.....	2.82
4666.75	II	39	.....	.....	2.82
4731.50	II	30	.....	.....	2.88

The Verweij[5] theoretical line profiles may also be used to obtain these initial parameters (even though the negative hydrogen ion contributes about half the observed opacity longward of the Balmer limit for a main-sequence A star). They indicated that our initial assumptions were of the correct order of magnitude for 95 Leonis.

The observed hydrogen line profiles for the subdwarfs are much narrower than are the Verweij profiles for an A-type star, unless the latter are computed for a surface gravity of the order of 10 cm/sec^2. Such a low acceleration of gravity seems to be ruled out, however, since the resulting damping constant gives a theoretical curve of growth that deviates greatly from the observed points. Moreover, for a star with log $g = 1.0$ and $T_{\text{eff}} = 8900°$ K, a sizable Balmer discontinuity is predicted, whereas the observed points on the curve of growth indicate that the absorption coefficient should be nearly constant across the Balmer limit. An alternative interpretation of the subdwarf profiles is that they indicate temperatures much lower than those of main-sequence A stars.

Thus, with approximate starting values of T_{eff} and log g, we read an initial estimate of the electron pressure from previously calculated curves[6] relating P_e, T, and g for an optical depth of 0.6. The gas pressure follows from tables[7] of P_g as a function of P_e and T. Finally, the damping constant (cf. eqs. [15], [16], and [17]) or, more specifically, the constant a (cf. eq. [21]), which is required in order to employ the correct theoretical curve of growth, was computed.

Wrubel's[8] theoretical curve of growth, based on Chandrasekhar's exact solution for a line profile in the Milne-Eddington model, is used throughout this paper. It consists of a plot of log $(Wc/\lambda v)$, where $v = (2kT/M)^{1/2}$ is the most probable velocity, against log η_0, the ratio of the line-absorption coefficient for zero damping to the continuous absorption coefficient at the center of the line. That is,

$$\eta_0 = \frac{\pi e^2}{m c} f \frac{c}{v\nu\pi^{1/2}} N \frac{1}{\kappa_\nu}, \tag{1}$$

where κ_ν is the effective continuous absorption coefficient, f is the oscillator strength, and N is the number of atoms in the lower level of the transition per gram of stellar material.

We define, for a given line, the quantity

$$f' = \frac{f(2J+1)}{\varpi_t}, \tag{2}$$

where J is the inner quantum number of the lower level of the transition and ϖ_t is the statistical weight of the entire lower term. Then we may write equation (1) as

$$\eta_0 = \frac{\pi e^2}{m c} f' \frac{c}{v\nu\pi^{1/2}} N_t 10^{-\theta(\chi-\chi_0)} \frac{1}{\kappa_\nu}, \tag{3}$$

where $\theta = 5040\ /T$, N_t is the total number of atoms per gram of stellar material in the lower term, and χ_0 is an arbitrary excitation potential to which we refer N_t. When a single curve of growth is to be used over different regions of the spectrum, the η_0 of equation (3) must be corrected to allow for the fact that

$$\frac{B^{(0)}}{B^{(1)}} = \frac{8}{3} \frac{kT_0}{h\nu} \frac{\kappa_\nu}{\bar{\kappa}} \tag{4}$$

[5] *Pub. Astr. Inst. Amsterdam*, No. 5, 1936.

[6] L. H. Aller, *Astrophysics* (Philadelphia: Blakiston Co., 1951), chap. vii.

[7] *Ibid.*, chap. iv. The $P_g(P_e, T)$ relation naturally depends on a particular choice of the chemical composition.

[8] *Ap. J.*, 109, 66, 1949.

varies with wave length. The necessary correction to log η_0 is tabulated as a function of $B^{(0)}/B^{(1)}$ by Wrubel.

King[9] has published absolute laboratory f-values for lines originating from several terms of *Fe* I. In the stars considered there are a number of these lines arising from the three terms $3d^64s^2\ a^5D$, $3d^7(^4F)4s\ a^5F$, and $3d^7(^4F)4s\ a^3F$ which have lower excitation potentials of about 0.00, 1.00, and 1.50 volts, respectively. Thus from the curve of growth we may obtain the relative numbers of atoms in each of the three terms and then employ the Boltzmann equation to find the excitation temperature.

Neglecting the lines that fall on the short-wave-length side of the Balmer limit, we may assume the continuous absorption to be nearly constant. Then, for a given star, equation (3) becomes

$$\log \eta_0 = \log \lambda + \log N_t - \theta(\chi - \chi_0) + \log f' + \text{const}. \tag{5}$$

From this expression we may obtain N_t.

Since $\chi - \chi_0$ is only a few hundredths of a volt for all the lines used, a small error in the value of θ will be insignificant. All the lines fall near the "flat" portion of the curve of growth, so slight uncertainties in the damping constant will not seriously affect the results, but the probable errors in the determination of θ_{exc} will be rather high. The excitation temperature turns out to be 5400° ± 900° K for both subdwarfs and 7500° ± 1100° K for 95 Leonis. The low excitation temperature of the subdwarfs suggests that their effective temperatures are lower than those for A stars, which is in agreement with our conclusions from the Verweij profiles. As we shall show later, the observed relative abundances of *Ca* II and *Ca* I, as determined from line profiles and equivalent widths, also indicate a temperature much lower than 8900° K. Thus a normal, high-surface-gravity, A-type atmosphere (either with a normal or with a low hydrogen content) seems to be an untenable assumption for the explanation of the subdwarf spectra.

IV. MODEL STELLAR ATMOSPHERES

For an accurate prediction of line profiles, a consideration of the variation with optical depth of temperature, electron pressure, gas pressure, and the mean absorption coefficient—i.e., a model atmosphere—is essential. The model atmosphere, however, is calculated for an assumed effective temperature and surface gravity, and the final model can be obtained only by a process of trial and error. That is, we assume values for the effective temperature and surface gravity and use the resulting model to predict the line profiles. Then a comparison between observed and computed profiles gives a clue as to the necessary modifications of our initial assumptions.

The structure of a model atmosphere depends on its assumed composition. In the cooler stars the hydrogen/metal ratio, A, is particularly important, since the metals supply the electrons. As long as the continuous absorption is primarily due to hydrogen, the value of A has little effect on the shapes of the hydrogen lines. The total intensities and the profiles of the metallic lines do depend on this ratio, however. We have tentatively adopted the hydrogen, helium, and metallic abundances as 1000, 200, and 0.44 by numbers of atoms. In Section VI we discuss the influence of the hydrogen/metal ratio upon the calcium-line profiles with the aid of a second subdwarf model atmosphere calculated for $\log A = 4.2$.

We can obtain a reasonably accurate initial approximation for 95 Leonis from the observed spectral type and absolute magnitude. Unfortunately, such estimates appear to be less helpful for the subdwarfs. The curve-of-growth method provides the starting approximation for the subdwarfs and serves as a check on the spectral-type estimates for 95 Leonis. A value of the ratio of *Fe* II to *Fe* I can be obtained from the curve of growth by utilizing Greenstein's η_0's for τ UMa in a manner explained in Section VII. This

[9] *Ap. J.*, **87**, 24, 1938; cf. also *ibid.*, **95**, 78, 1942.

leads, by virtue of the Saha equation, to a relation between the temperature and electron pressure at a representative point in the stellar atmosphere, viz.,

$$\theta I + \log P_e = F(\theta) . \tag{6}$$

Here I is the ionization potential of *Fe*, and F is nearly constant over a small range of θ. Another such relation could be obtained from similar considerations of another element, were the data of sufficient accuracy. In practice, however, as Greenstein[10] has pointed out, two such equations give straight lines so nearly parallel that the solution is essentially indeterminate.

In the wave-length region considered (λλ 4000–4800), κ_ν is very nearly constant. Therefore, in computing η_0 we may assign some arbitrary value to κ_ν so that the relation of the individual points on the empirical curve of growth will be nearly correct, although the zero point on the η_0-scale will be arbitrary. Now an assumption as to the abundance of *Fe* will give us the zero point (from a comparison of the observed and theoretical curves) and hence κ_ν. Greenstein[11] has tabulated $\kappa_\nu (H + H^-)$ as a function of θ and $\log P_e$ at λ 4300. Thus, with a value for κ_ν obtained from fixing the η_0 zero point, we

TABLE 3

PROVISIONAL MODEL ATMOSPHERES

τ	95 LEONIS $T_{\text{eff}} = 8900$, $\log g = 3.90$				SUBDWARFS $T_{\text{eff}} = 6300$, $\log g = 4.80$			
	T	$\log \bar{\kappa}$	$\log P_g$	$\log P_e$	T	$\log \bar{\kappa}$	$\log P_g$	$\log P_e$
0.05....	7440	−0.08	+2.70	+1.26	5250	−0.70	+4.50	+0.90
0.10....	7610	+0.05	+3.10	+1.60	5440	−0.61	+4.60	+1.07
0.20....	7970	+0.38	+3.33	+1.93	5640	−0.48	+4.76	+1.27
0.40....	8460	+0.69	+3.48	+2.30	6000	−0.28	+4.94	+1.59
0.60....	8840	+0.90	+3.54	+2.47	6280	−0.10	+5.05	+1.87
0.80....	9130	+1.08	+3.57	+2.60	6570	+0.07	+5.10	+2.14
1.00....	9440	+1.25	+3.59	+2.72	6900	+0.20	+5.13	+2.30
2.00....	10610	+1.45	+3.63	+3.08	7580	+0.55	+5.20	+2.70
3.00....	11480	+1.40	+3.65	+3.20	8120	+0.80	+5.24	+3.00

can find another relation between θ and $\log P_e$ which may be solved simultaneously with equation (6). If we take the representative point for the formation of *Fe* lines to be $\tau = 0.25$, since iron becomes rapidly ionized with increasing optical depth, then approximately $\theta_{\text{eff}} = \theta(0.6) = 0.90\,\theta(0.25)$ and, very roughly, $P_e(0.6) = 2.5\,P_e(0.25)$. The numerical values for θ_{eff} and P_e (0.6) may then be utilized to predict the surface gravity.[8]

The method is admittedly crude: a small error in the empirical *Fe* II/*Fe* I abundance ratio will be rather serious. Also the resulting effective temperature and surface gravity will depend upon our assumption as to the total *Fe* abundance; hence the method is even less reliable when applied to the subdwarfs, where peculiar abundances might well prevail.

Nevertheless, the results did tend to substantiate the assumed effective temperature and surface gravity for 95 Leonis and sustained our suspicions of a low temperature and high surface gravity for the subdwarfs. But it must be emphasized that the trial-and-error approach by the method of model atmospheres was necessary for an accurate representation of line profiles. The final effective temperatures and surface gravities are given in Table 3 with the results of the numerical integrations for the respective models. The predicted surface gravities may well be in error by a factor of 2 or 3.

[10] *Ap. J.*, **107**, 151, 1948.

[11] *Ibid.*, Table 10.

The variation of temperature with optical depth depends upon the physical process involved in the transfer of energy through the stellar atmosphere. We have assumed radiative equilibrium for our present calculations. B. Strömgren[12] has suggested that the temperature dependence for convective equilibrium is probably not greatly different from that for radiative equilibrium in an A dwarf atmosphere.

We start by assuming the atmosphere to be in hydrostatic equilibrium:

$$\frac{dP_g}{d\tau} = \frac{g_e}{\bar{\kappa}(P_e, T)} . \tag{7}$$

In equation (7) g_e is the effective surface gravity and for these stars should differ little from that calculated from the mass and radius, and $\bar{\kappa}$ is the Chandrasekhar mean absorption coefficient.[13] The temperature dependence upon optical depth is given by Chandrasekhar's exact solution of the equation of radiative transfer for a stellar atmosphere in radiative equilibrium.[14]

In the evaluation of $\bar{\kappa}$ we have made the simplifying assumption that the variation of flux distribution, F_ν/F, is so small throughout the relevant layers that it may be taken as constant with optical depth and equal to the value at $\tau = 0.6$. Thus we may use the values of the mean absorption coefficient per gram of hydrogen, $\bar{\kappa}(H + H^-)$, tabulated for various temperatures and electron pressures by Chandrasekhar and Münch.[15] The effects of electron scattering are negligible for A-type dwarfs within the limits of accuracy of our theory.

The calculation of the model atmosphere is executed in a straightforward fashion, the initial approximation being obtained in a manner similar to that described by Unsöld.[16] Once $P_g(\tau)$ is obtained, P_e may be found immediately from the afore-mentioned tables of $P_e(P_g, T)$.

Were the observational data of sufficient accuracy to merit the labor involved, the model atmospheres presented here could be refined by a calculation of the mean absorption coefficient that takes account of the variation of flux distribution with depth.

V. HYDROGEN-LINE PROFILES

We now wish to determine whether the narrow hydrogen lines in the two subdwarfs may be satisfactorily represented in terms of a normal hydrogen content and a temperature characteristic of an F-type (rather than an A-type) star.

Although the observed profiles of corresponding lines in the two subdwarfs differ somewhat from one another, the differences are no more than might be explained by observational error. In the subdwarfs we would expect greater residuals between observed and computed profiles, which are based on one plate for each star, than in 95 Leonis, for which profiles were obtained from two grating plus two prism plates. Consequently, the subdwarfs have been considered together, and their computed profiles are based on the same model atmosphere. In general, the data for HD 19445 are probably more reliable than those for HD 140283, since the coudé plate of the latter star was somewhat underexposed for spectrophotometric purposes in the region studied.

The principal source of line broadening for stellar hydrogen lines is the linear Stark effect. According to the Holtsmark theory of statistical broadening, at a point in the line well removed from the Doppler core, the line-absorption coefficient will be

$$l(\Delta\lambda) = N_2 a(\Delta\lambda) = N_2 3\,2\,1 C_n P_e T^{-1} (\Delta\lambda)^{-5/2} . \tag{8}$$

[12] Private communication.

[13] See S. Chandrasekhar, *Radiative Transfer* (Oxford: Clarendon Press, 1950), p. 298, eq. (46).

[14] *Ibid.*, p. 294, eq. (31); also *ibid.*, p. 80, Table X.

[15] *Ap. J.*, **104**, 446, 1946.

[16] *Physik der Sternatmosphären* (Berlin: J. Springer, 1938), p. 144.

Here C_n is a constant computed from the Stark-effect theory for each hydrogen line, and N_2 is the number of atoms in the second level of hydrogen per gram of stellar material.

The theory of line profiles on the basis of the Milne-Eddington model, where $\eta_\nu = l_\nu/\kappa_\nu$ is constant with the depth, has been given by A. S. Eddington,[17] B. Strömgren,[18] and by S. Chandrasekhar,[19] who has obtained an exact solution for $r_\nu = F_L(0)/F_c(0)$, the ratio of the flux at a point in the line to the continuous flux in the near-by continuum. When η_ν undergoes small variations, the residual intensity may be found by the mean-value method suggested by Strömgren and modified by M. Tuberg[20] to the problem of the center-limb variation of a number of lines of the solar spectrum.

In the model atmospheres presented in Table 3, η_ν for the hydrogen and calcium lines varies rapidly with optical depth, and approximate methods no longer suffice. Therefore, we have used a method proposed by Strömgren wherein the differential equation of transfer (with its boundary conditions) is replaced by an integral equation. The solution is obtained by an iteration procedure and in such a manner that the detailed variations of η_ν with depth are taken into account.

Theoretical line profiles depend upon the quantity ϵ, which is a measure of the relative importance of scattering and thermal absorption in the process of line formation. For monochromatic radiative equilibrium (pure scattering), $\epsilon = 0$; and for the limiting case of local thermodynamic equilibrium, $\epsilon = 1$. Since a complete theory of line formation is not yet available, it is necessary to use an empirical ϵ. Let us define

$$\mu_\nu = \frac{1}{1+\eta_\nu} \tag{9}$$

and

$$\Lambda_\nu = \frac{1+\epsilon\eta_\nu}{1+\eta_\nu}. \tag{10}$$

At the center of a line η_ν becomes large and $\Lambda \to \epsilon$. Hence, using the Milne-Eddington formula in Chandrasekhar's first approximation, viz.,

$$r_\nu = \frac{2}{(4/3)\sqrt{3} + (1/2)(x_0/n_\nu)} \frac{(4/3)\sqrt{(3\Lambda_\nu)} + (1/2)(x_0/n_\nu)\mu_\nu}{(1+\sqrt{\Lambda_\nu})}, \tag{11}$$

we find, for $\Delta\lambda = 0$,

$$r_0 = \frac{2}{(4/3)\sqrt{3} + (1/2)(x_0/n_\nu)} \frac{(4/3)\sqrt{(3\epsilon)}}{(1+\sqrt{\epsilon})}. \tag{12}$$

In equations (11) and (12)

$$n_\nu = \frac{\kappa_\nu}{\bar{\kappa}} \tag{13}$$

and

$$x_0 = \frac{h\nu}{kT_0}(1 - e^{-h\nu/kT_0})^{-1}, \tag{14}$$

where T_0 represents the boundary temperature.

[17] *M.N.*, **89**, 620, 1929.

[18] *Ap. J.*, **86**, 1, 1937; cf. also *Festschrift für Elis Strömgren* (Copenhagen: Einer Munksgaard, 1940), p. 218.

[19] *Ap. J.*, **106**, 145, 1947.

[20] *Ap. J.*, **103**, 145, 1946.

If we use the observed residual intensity at the center of the line, we can solve equation (12) for ϵ. This method is very sensitive, however, to errors in the boundary temperature and in n_ν, which must be taken near the top of the atmosphere. Also the empirical measures of the central intensity, r_0, have a fairly large probable error, for reasons explained in Section II. Therefore, we have computed profiles for 95 Leonis with various assumed values of ϵ and find that with the adopted model atmospheres a value of $\epsilon \sim 0.25$ gives a good representation of the three lines, $H\beta$, $H\gamma$, and $H\delta$. For the subdwarfs it turns out that the choice of ϵ is not so critical, and computations for $\epsilon = 0$ and $\epsilon = 1$ give very nearly the same profiles in the damping wings. From considerations of the process of line formation, it seems likely that $\epsilon \sim 1$ for hydrogen lines.

In Tables 4 and 5 and Figures 2–7 we compare the observed profiles with those com-

TABLE 4

HYDROGEN PROFILES FOR 95 LEONIS

Δλ (A)	$H\beta$		$H\gamma$		$H\delta$	
	Obs. r_λ	Comp. r_λ	Obs. r_λ	Comp. r_λ	Obs. r_λ	Comp. r_λ
5.....	0.54	0.55	0.49	0.50	0.47	0.47
10.....	.72	.71	.70	.72	.67	.70
15.....	.82	.81	.83	.85	.81	.84
20.....	0.90	0.90	0.91	0.93	0.90	0.92

TABLE 5

HYDROGEN PROFILES FOR SUBDWARFS

Δλ (A)	$H\beta$			$H\gamma$			$H\delta$		
	Obs. r_λ		Comp. r_λ	Obs. r_λ		Comp. r_λ	Obs. r_λ		Comp. r_λ
	HD 19445	HD 140283		HD 19445	HD 140283		HD 19445	HD 140283	
1.0.....	0.63	0.65	0.68	0.61	0.68	0.65	0.65	0.63	0.65
2.0.....	.78	.80	.81	.76	.81	.75	.79	.75	.78
3.0.....	.85	.86	.86	.84	.87	.83	.87	.83	.86
4.0.....	0.88	0.90	0.90	0.89	0.93	0.90	0.91	0.90	0.91

puted by Strömgren's iteration method. Values of r_ν were not computed near the line center, where the error arising from the uncertainty in ϵ enters to the fullest extent. In the wings the agreement appears to be satisfactory.

VI. THE CALCIUM ABUNDANCE

The determination of the abundances of the elements in a stellar atmosphere may proceed along two different lines. One is a comparison of theoretical and observed equivalent widths; the other is an analysis of the line profiles. An example of the first method is the curve-of-growth procedure, which makes possible the utilization of a large number of lines but which frequently involves the introduction of questionable assumptions; e.g., η_ν is assumed constant with depth. The strongest line arising from *Ca* I—λ 4227—is so narrow that only the instrumental profile is obtained. Therefore, the best alternative

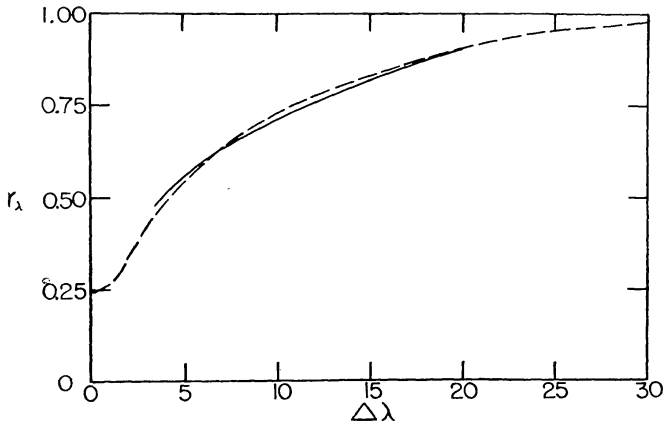

FIG. 2.—Profile of $H\beta$ in 95 Leonis. *Dashed curve*, observed; *solid curve*, computed

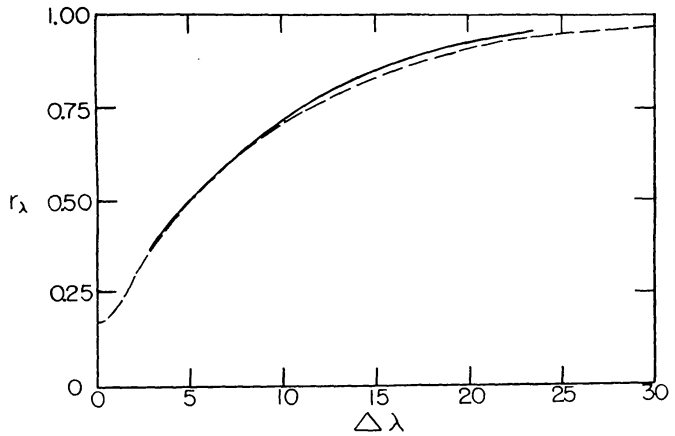

FIG. 3.—Profile of $H\gamma$ in 95 Leonis. *Dashed curve*, observed; *solid curve*, computed

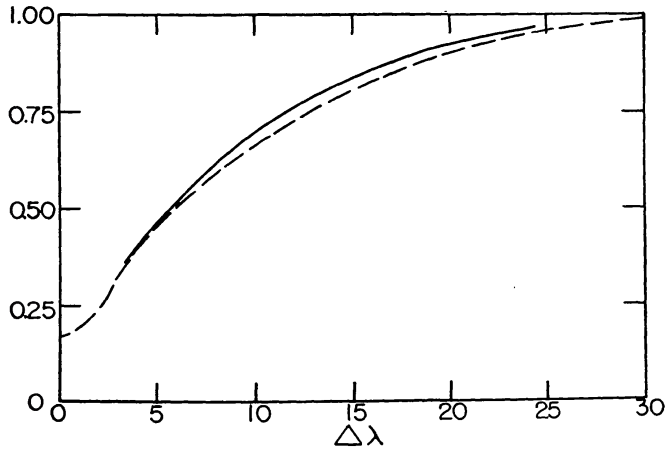

FIG. 4.—Profile of $H\delta$ in 95 Leonis. *Dashed curve*, observed; *solid curve*, computed

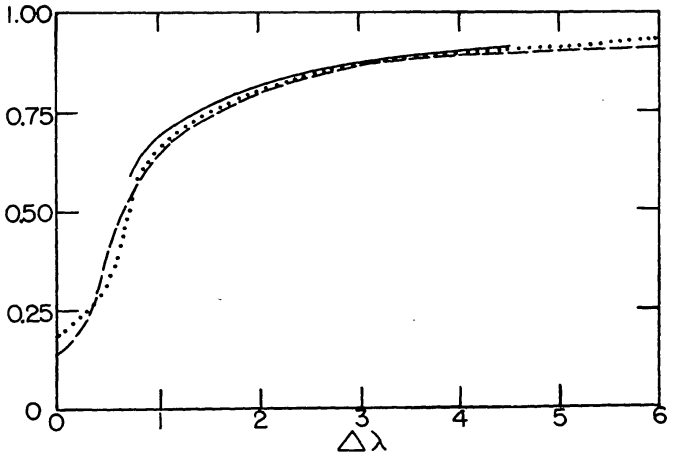

FIG. 5.—Profiles of $H\beta$ in subdwarfs. *Dashed curve*, observed in HD 19445; *dotted curve*, observed in HD 140283; *solid curve*, computed.

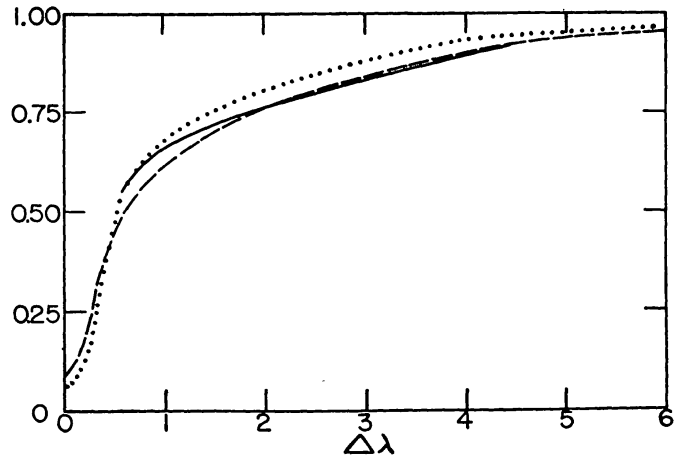

FIG. 6.—Profiles of $H\gamma$ in subdwarfs. *Dashed curve*, observed in HD 19445; *dotted curve*, observed in HD 140283; *solid curve*, computed.

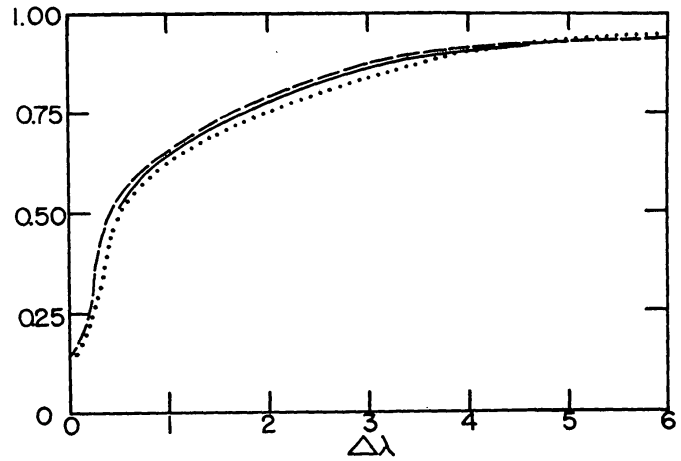

FIG. 7.—Profiles of $H\delta$ in subdwarfs. *Dashed curve*, observed in HD 19445; *dotted curve*, observed in HD 140283; *solid curve*, computed.

to calculate the theoretical profile, taking the variation of η_ν with τ into account, and to compare the theoretical with the observed equivalent width.

The second method is generally preferable when a model atmosphere is available and the line to be analyzed is wide enough that it is but little affected by the finite resolving power of the spectrograph. The K line of *Ca* II offers an excellent opportunity for such an analysis. Since both λ 3933 and λ 4227 are resonance lines, we may adopt $\epsilon = 0$, corresponding to pure scattering. Theoretical *f*-values have been calculated for both lines.[21]

For λ 3933 we have taken values of Δλ well removed from the Doppler core, as we did for the hydrogen lines. Then there are three sources of line broadening that must be considered: the quadratic Stark effect (electron damping), collisional damping, and radiation (natural) damping. The first two damping constants may be calculated from Weisskopf's single-encounter theory. For the electron damping in *Ca* II we use the formula of M. Rudkjøbing:[22]

$$\Gamma_{\rm el} = 10^{-4.46} \times 0.72 N_e T^{-1/2} . \tag{15}$$

TABLE 6

COMPARISON OF K-LINE PROFILES WITH ASSUMED CALCIUM ABUNDANCES

Δλ (A)	95 Leonis		HD 19445		HD 140283	
	Obs. r_λ	Comp. r_λ $Ca(*)/Ca\ \odot =$ 1.0	Obs. r_λ	Comp. r_λ $Ca(*)/Ca\ \odot =$ 0.040	Obs. r_λ	Comp. r_λ $Ca(*)/Ca\ \odot =$ 0.025
1.0.....	0.48	0.47	0.18	0.25	0.38	0.40
2.0.....	.79	.81	.62	.63	.72	.73
3.0.....	.89	.90	.80	.80	.89	.90
4.0.....	0.94	0.95	0.89	0.88	0.97	0.97

From Lindholm's[23] expression for collisional damping we obtain, for λ 3933,

$$\Gamma_{\rm coll} = 10^{+6.92} P_g T^{-0.70} . \tag{16}$$

Formulae similar to equations (15) and (16) hold for λ 4227. Also for resonance lines we may write

$$\Gamma_{\rm rad} = A_{nn'} , \tag{17}$$

where $A_{nn'}$ is the Einstein coefficient of spontaneous emission.

In the damping wings the absorption coefficient per atom is given by

$$a_\lambda = 16.5 \times 10^{-26} f_{n'n} \frac{\Gamma \lambda^2}{\gamma_{el} (\Delta\lambda)^2} , \tag{18}$$

where $\Gamma = \Gamma_{\rm el} + \Gamma_{\rm coll} + \Gamma_{\rm rad}$. The profiles were computed by the iteration procedure mentioned in the preceding section. An adopted abundance of 1.36×10^{18} calcium atoms per gram of stellar material represents the profiles in 95 Leonis as well as in the sun. On the other hand, values of 0.040 and 0.025 times the solar abundance are necessary in order to explain the relatively sharp *Ca* II lines for the subdwarfs. Table 6 and Figures 8–10 show a comparison of theoretical and observed profiles.

[21] D. R. and W. Hartree, *Proc. R. Soc. London, A*, **164**, 161, 1938.

[22] *Ann. d'ap.*, **12**, 237, 1949.

[23] *Ark. f. Math., Astr., och Phys.*, Vol. **28**, No. 3, 1941.

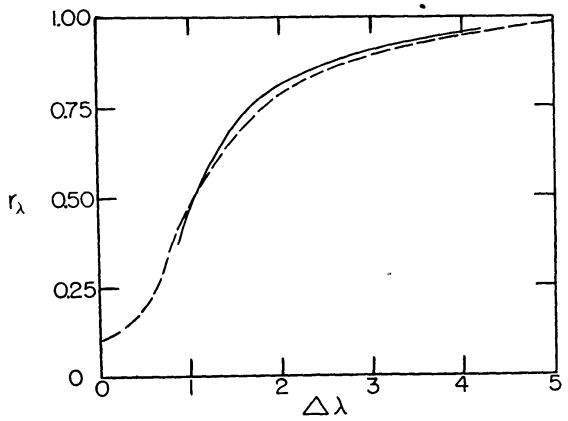

FIG. 8.—Profile of K line in 95 Leonis. *Dashed curve*, observed; *solid curve*, computed for solar abundance of *Ca*.

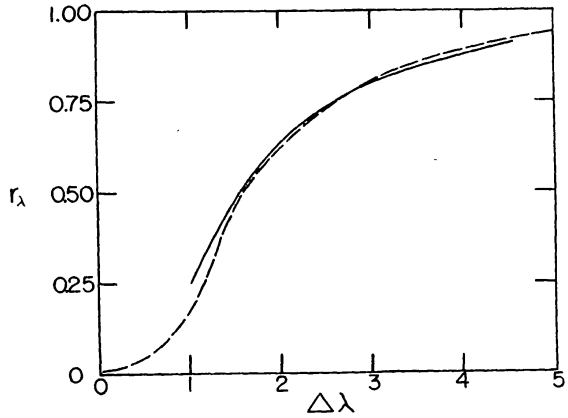

FIG. 9.—Profile of K line in HD 19445. *Dashed curve*, observed; *solid curve*, computed for 0.040 × solar abundance of *Ca*.

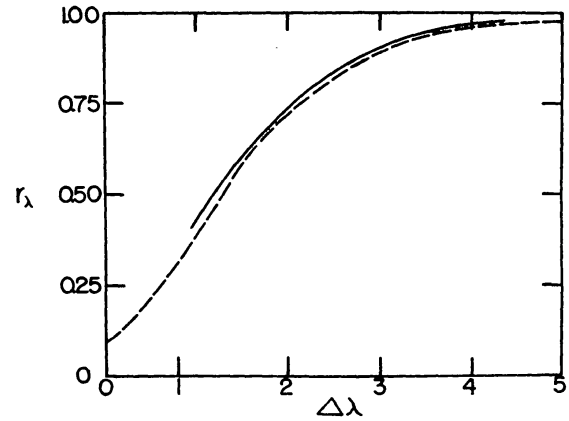

FIG. 10.—Profile of K line in HD 140283. *Dashed curve*, observed; *solid curve*, computed for 0.025 × solar abundance of *Ca*.

In calculating the theoretical equivalent width of λ 4227, we must consider the Doppler core. Define

$$u = \frac{\Delta\lambda}{b_\lambda}, \tag{19}$$

where b_λ is the Doppler width given by

$$b_\lambda = \frac{\lambda v}{c}, \tag{20}$$

and v is the most probable velocity. Let

$$a = \frac{\Gamma c}{4\pi\nu^2}\frac{1}{b_\lambda} = \frac{\Gamma\lambda}{4\pi v}, \tag{21}$$

so that by equations (19) and (21) we can calculate u and a for various points in the model atmosphere. Then

$$\frac{\alpha_\nu}{\alpha_0} = H_0(u) + aH_1(u) + a^2H_2(u) + \ldots \tag{22}$$

is computed from the tables of $H(u)$ given by D. Harris,[24] where

$$\alpha_0 = \frac{\pi e^2}{mc} f \frac{c}{v\nu\pi^{1/2}}. \tag{23}$$

Physically, α_0 is the absorption coefficient at the line center for zero damping. The line profile may now be calculated as before. In Table 7 we have listed the observed and

TABLE 7

OBSERVED AND COMPUTED INTENSITIES FOR λ 4227 *Ca* I

Star	W Obs.* (mA)	W Comp. (mA)	Assumed $Ca^{(*)}/Ca\ \odot$
95 Leonis.....	130	124	1.0
HD 19445.....	230	230	0.036
HD 140283....	154	154	0.013

* Observed equivalent widths corrected for grating scattering.

theoretical equivalent widths for λ 4227 and the abundance assumed for the calculations. Table 8 presents the abundance of *Ca* as obtained from *Ca* II and *Ca* I, with a mean value computed with a weight of 2 for *Ca* II and of 1 for *Ca* I determinations, since the former involved line profiles rather than equivalent widths and are considered more reliable. The agreement between the two determinations seems satisfactory, considering the fact that the subdwarf data are based on only one plate. The fact that the two values are similar in both cases further suggests that our model atmospheres, which were accepted because they satisfactorily predicted the shapes of the hydrogen lines, are approximately correct. We must emphasize that the model atmospheres (Table 3) and the subsequent abundance determinations in Table 8 depend on the assumed composition. $H/He = 5$, and $\log A = 3.36$. An increase in the hydrogen/metal ratio will modify the calcium abundance determination. To investigate this point, we have calculated a model atmosphere for $T_{\text{eff}} = 6300°$ K and $\log g = 4.80$ for the case of $\log A = 4.20$ and no

[24] *Ap. J.*, **108**, 112, 1948.

helium. For this purpose we have employed B. Strömgren's P_g, P_e tables[25] and the more recent data on the continuous absorption coefficient.[15] With this model atmosphere the K-line profile in HD 19445 may be fitted with a profile calculated for a calcium abundance of about 40 per cent of the previous value.

VII. THE CURVE OF GROWTH FOR IRON

In order to calculate the log (η_0/N)'s by equation (1), we must have reliable f-values. Theoretical strengths are poor, particularly for *Fe* II, although some progress has been made for *Fe* I. Laboratory f-values are available for some transitions arising from the lower terms in *Fe* I, and it is hoped that data will eventually be available for lines involving the higher levels and for *Fe* II.

Until such material is forthcoming, we are forced to use empirical data based on solar or stellar curves of growth. The usual procedure has been to construct an initial curve of growth with the aid of lines for which relative f-values are known, usually lines of *Fe* I, *Ti* I, etc. Then, using the observed equivalent widths, on the assumption that the same curve of growth holds for all atoms and ions, we read empirical relative f-values from the curve. This procedure is objectionable for a number of reasons, among which we

TABLE 8

SUMMARY OF CALCIUM AND IRON ABUNDANCE DETERMINATIONS

Star	$N(*)/N(\odot)$					
	Calcium			Iron		
	λ 4227	λ 3933	Weighted Mean	*Fe* I	*Fe* II	Weighted Mean
95 Leonis	1.0+	1.00	1.00	0.68	1.25	0.97
HD 19445	0.036	0.040	0.039	.13	0.30	.17
HD 140283	0.013	0.025	0.021	0.06	0.18	0.09

may enumerate the following: (1) Because of the differences in excitation, the effects of blending, and secondary effects such as interlocking, empirical f-values derived for the solar atmosphere are not necessarily valid for hotter stars. (2) Higher-excitation lines originate, on the average, in deeper layers of the star, where the collisional damping is greater. In particular, the *Fe* II lines are formed in deeper, hotter, denser layers than are the *Fe* I lines in the sun. Thus spuriously large f-values for transitions involving high levels may be found.[26] (3) Turbulence may not be properly taken into account in the construction of solar and stellar curves of growth. Furthermore, it may depend on the optical depth. On the basis of turbulence considerations, Unsöld and Struve[27] have recently questioned the validity of solar-line strengths derived with an excitation temperature as low as 4800° K.

Greenstein has overcome some of these difficulties by the use of empirical strengths in F stars.[10] His procedure was to construct a curve of growth for τ UMa with solar strengths and then to obtain empirical strengths for the lines in this star from the adopted curve of growth. The τ UMa empirical strengths were used in the construction

[25] "Tables of Model Stellar Atmospheres," *Pub. Medd. Københavns Obs.*, No. 138, Table 7, 1944.

[26] E.g., see A. K. Pierce and L. Goldberg, *Technical Report No. 2* (ONR Contract N6onr-232-V [1948]), pp. 7–14.

[27] *Ap. J.*, **110**, 455, 1949.

of curves of growth for other F stars. Although some of the obstacles noted under objection 1 above are circumvented by this procedure, complications introduced by stratification are not so easily avoided. Ultimately, Greenstein's η_0's for τ UMa[28] and his recently determined η_0's for υ Sgr, which we have used in the construction of the curves of growth for *Fe* I and *Fe* II, are based on the solar data.

The η_0's for υ Sgr (denoted here by η_0'') were reduced to the same system as those for τ UMa (which we represent by η_0') in the following manner: Writing equation (1) for a given line in each star and taking the ratio of the two equations, we have

$$\frac{\eta_0''}{\eta_0'} = \frac{v'B'(T)\, N_0''\, \kappa_\nu'}{v''B''(T)\, N_0'\, \kappa_\nu''}\, 10^{-(\theta''-\theta')\chi}. \tag{24}$$

Here $B(T)$ represents the partition function and N_0 the number of atoms in the stage of ionization in question. Also in equation (24) we have made use of the Boltzmann equation,

$$N = \frac{N_0 \varpi}{B(T)}\, 10^{-\theta\chi}. \tag{25}$$

Since the continuous absorption coefficients are nearly constant in both stars over the wave-length region in which the η_0'''s are listed by Greenstein ($\lambda\lambda$ 4000–4800), we may write equation (24), considering only lines with nearly the same value of χ,

$$\log \eta_0'' = \log \eta_0' + \text{const}. \tag{26}$$

For *Fe* II, 19 lines with $\chi \sim 2.75$ volts were found in common in τ UMa and υ Sgr; thus the constant in equation (26) could be determined. Then a few additional η_0'''s were converted to η_0''s. For *Fe* I all the η_0's were taken only from τ UMa. In general, the η_0's obtained from τ UMa were given more weight in fixing the η_0's for the stars considered in this paper.

The η_0'''s are related to the η_0's of 95 Leonis or of the subdwarfs by an equation similar to (24) in which we replace η_0'' by η_0. Similarly, we use unprimed symbols for the other quantities involved when they pertain to the star in question. Defining

$$z = \frac{N_0}{N_0'}, \tag{27}$$

we obtain

$$\frac{\eta_0}{z} = \eta_0'\, \frac{v'B'(T)\, \kappa_\nu'}{vB(T)\, \kappa_\nu}\, 10^{-(\theta-\theta')\chi}. \tag{28}$$

The numerical values of the factors pertaining to τ UMa can be obtained from the data given by Greenstein. We evaluate the necessary data for 95 Leonis and the subdwarfs at an optical depth $\tau = 0.25$, and calculate $\log \eta_0/z$ for each line. The correct branch of Wrubel's[8] theoretical curve of growth is obtained from the value of $\log a$ given by equation (21). Thus the *Fe* I and *Fe* II curves of growth provide values of z^{I} and z^{II}, respectively.

Since τ UMa was found to have about the same iron abundance as the sun and since in all the stars involved *Fe* is almost entirely in the singly ionized stage,

$$z^{\text{II}} = \frac{N_0(Fe\ \text{II})}{N_0'(Fe\ \text{II})} = \frac{Fe}{Fe\ (\odot)}. \tag{29}$$

[28] *Op. cit.*, Table 2.

gives directly a value of the abundance of iron in the star. In order to derive a value of the total *Fe* abundance from the *Fe* I curve of growth, we must obtain a relation between z^{I} and z^{II} by means of the Saha equation. On the basis of model-atmosphere considerations for a metal that becomes rapidly ionized with depth, we take $\theta_{\mathrm{ion}} = \theta(\tau = 0.25)$. Furthermore, we use the value

$$\log \frac{Fe\,\mathrm{I}(\odot)}{Fe\,(\odot)} = -1.04\,,$$

which is based on a temperature of 5675° K and log $P_e = 1.51$ dyne/cm² for the solar reversing layer.

The curves of growth for the three stars are given in Figures 11–13. The number of *Fe* II lines available in the subdwarfs was small. Consequently, in fixing the total abundance of *Fe*, we gave the abundance determinations from the *Fe* II curves of growth one-third the weight of the determinations based on *Fe* I (cf. Table 8).

Although for 95 Leonis the mean value of the *Fe* abundance turns out to be very nearly the solar value, the separate determinations for *Fe* I and *Fe* II differ by a factor of 2. In fact, for all three stars the abundance found from *Fe* II is consistently higher by a factor of from 2 to 3.

Attempts to determine the *Ca* abundance from the curve of growth gave discrepancies, similar to those of *Fe*, which were much higher than the differences found in the calculation of profiles. These discrepancies, although not larger than one usually encounters in the curve-of-growth type of analysis, still are undesirable. Perhaps the difficulty is inherent in the method, which forces us to represent atoms in two stages of ionization by the same effective optical depth. In spite of the large probable error in the subdwarf curves of growth, the observed *Fe* abundance appears to be smaller than in the sun, although this conclusion must be taken with caution.

VIII. PREDICTION OF COLOR TEMPERATURES AND BALMER DISCONTINUITIES

The color temperature of a star is obtained by fitting a Planckian curve to the intensity-curve of the star over a given wave-length region. That is, the average slope of the Planck black-body-curve for $T = T_c$ must be the same as that for the true energy distribution-curve in this interval. If F_1 and F_2 denote the emergent fluxes at wave lengths λ_1 and λ_2 and if we employ the Wien approximation to the Planck formula, the color temperature T_c is given by

$$T_c = \frac{c_2 (\log_{10} e)\ (1/\lambda_2 - 1/\lambda_1)}{\log F_1/F_2 - 3 \log \lambda_2/\lambda_1}, \tag{30}$$

where c_2 is the second Planck radiation constant.

The ratio F_1/F_2 may be calculated from the model atmosphere, since the Planck function, $B_\nu(T)$, is known for all optical depths, τ_ν. For a body that is not in thermodynamic equilibrium, the color temperature may differ greatly from the effective temperature. Also, for a star in which there are significant departures from gray-body energy distribution, the color temperature may vary considerably with the spectral region for which it is evaluated. Observations of color temperatures by the Greenwich observers[29] and by Barbier and Chalonge[30] have been made in regions of the spectrum above λ 4000. Accordingly, we have computed the color temperatures for these stars in the wave-length interval 4100–5500 A.

[29] Sir F. Dyson, *Observations of Color-Temperatures of Stars, 1926–1932* (London, 1932); also *M.N* **100**, 189, 1940.

[30] *Ann d'ap.*, **4**, 30, 1941.

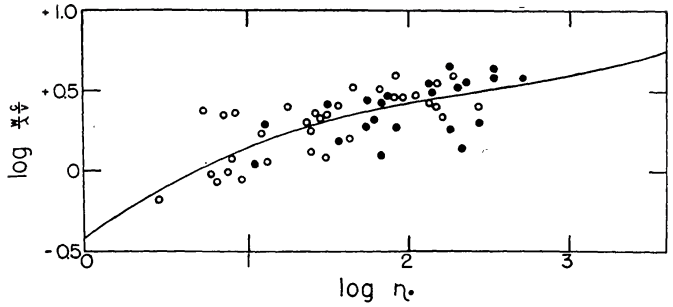

FIG. 11.—Curve of growth for 95 Leonis. *Open circles, Fe* I; *closed circles, Fe* II. The line is the theoretical curve.

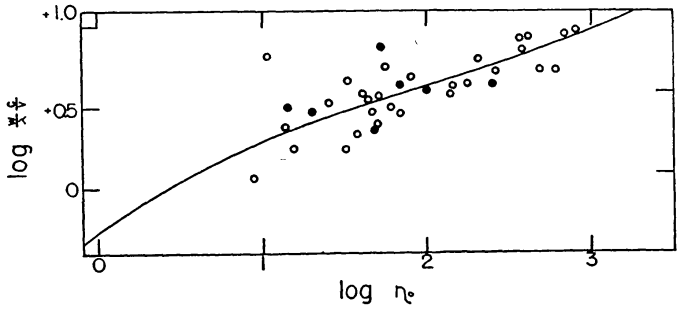

FIG. 12.—Curve of growth for HD 19445. *Open circles, Fe* I; *closed circles, Fe* II. The line is the theoretical curve.

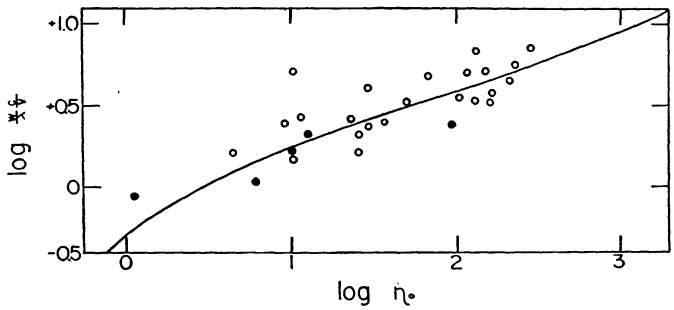

FIG. 13.—Curve of growth for HD 140283. *Open circles, Fe* I; *closed circles, Fe* II. The line is the theoretical curve.

The Balmer discontinuity is calculated directly from the defining equation,

$$D = \log \frac{F_{\lambda>3647}}{F_{\lambda<3647}}. \tag{31}$$

At present, no measures of T_c or D are available for these stars. The predicted values are tabulated in Table 9, along with our determinations of the excitation, ionization, and effective temperatures.

IX. CONCLUSION

95 Leonis appears to be a normal A-type star, whose spectrum may be satisfactorily interpreted by means of a model atmosphere for a star in radiative equilibrium and with normal abundances. On the other hand, our two so-called "A-type subdwarfs" may evidently be satisfactorily represented by an F-type subdwarf model atmosphere. Observational checks of the color temperatures and Balmer discontinuities presented in Table 9 are certainly to be desired, but, in the light of the present evidence, effective temperatures of around 6300° K seem probable.

The one possibly undesirable factor in our interpretation is the prediction of abnormally small amounts of *Ca* and *Fe*. Low apparent abundances of some elements are

TABLE 9

COMPARISON OF STELLAR TEMPERATURES AND BALMER DISCONTINUITY

Star	T_{eff}	T_{ion}	T_{exc}	T_c	D
95 Leonis.....	8900	8100	7500	16,000	+0.64
Subdwarfs.....	6300	5700	5400	8250	+0.16

not a new phenomenon for F stars. Greenstein[31] has recently found very large apparent deficiencies of *Ca* in the metallic-line stars. In fact, it was the abnormally sharp K line in these stars, combined with fairly wide hydrogen lines, that caused the metallic-line stars to be originally classified in spectral type A.

As Greenstein suggests, the observed deficiency of some elements could possibly be caused by *excess* second ionization—i.e., much higher ionization than that predicted by the Saha formula. For example, an unusually large amount of ultraviolet radiation of the right frequencies might not affect the first ionization of calcium but might place most of the atoms in the unobservable stage of *Ca* III, leaving the ratio of *Ca* II/*Ca* I unaffected. Rudkjøbing[32] has suggested that the apparent peculiar abundances in the metallic-line stars are a result of a difference in atmospheric structure between the metallic-line and the "normal" F stars. In the subdwarf model given in Table 3, convection would appear to set in[33] at about $\tau \sim 1$. According to Rudkjøbing, a large surface gravity will tend to suppress adiabatic equilibrium in the convection zone; this might have the effect of causing excess ionization. At any rate, the stars treated in the present paper are undoubtedly quite different from the metallic-line stars, and it may well be that superionization cannot explain the apparent peculiar abundances found in these subdwarfs.

The determination of the calcium abundance, based on the theoretical line profiles, is probably more accurate than the iron abundance, determined by the curve-of-growth method. Although many workers have previously suspected the subdwarfs of having a

[31] *Ap. J.*, **109**, 121, 1949. [32] *Ann. d'ap.*, **13**, 69, 1950. [33] See Unsöld, *op. cit.*, p. 381.

low hydrogen content, it appears that, with respect to *Ca* and *Fe* at least, the subdwarfs are *rich* in hydrogen! The extent and accuracy of our data did not suffice for the construction of curves of growth for elements other than *Fe*. The determinations of other metallic abundances in the subdwarfs would be most interesting. Also an analysis of subdwarfs of other spectral types would do much toward determining whether a large hydrogen/metal ratio exists in type II population objects in general.

A recent investigation of high- and low-velocity F dwarfs by M. and B. Schwarzschild[34] indicated that the *H/Fe* ratio might be somewhat larger in the high-velocity dwarfs than in the low-velocity dwarfs, although the results were rather uncertain. Miss N. Roman[35] has recently published a list of weak-lined F and G stars that are probably closely related to the subdwarfs considered here. If, indeed, this turns out to be the case, then Miss Roman's weak-lined stars may be classified systematically too early.

We are indebted to Dr. R. F. Sanford for making available to us his coudé plates of 95 Leonis and the two subdwarfs. Thanks are due to Dr. J. L. Greenstein, who supplied us with empirical line strengths from υ Sgr in advance of publication, and to Mrs. Chamberlain, who made the accompanying line drawings.

[34] *Ap. J.*, **112**, 248, 1950.

[35] *Ap. J.*, **112**, 554, 1950.